Received: 14 March 2023 | Revised: 24 January 2024 | Accepted: 17 February 2024

IET Quantum Communication

DOI: 10.1049/qtc2.12091

The Institution of Engineering and Technology WILEY

ORIGINAL RESEARCH

The impact of spot-size on single-photon avalanche diode timing-jitter and quantum key distribution

Alexandra Lee[1,2] | Alfonso Tello Castillo[2] | Craig Whitehill[1] | Ross Donaldson[2]

[1]Wideblue Ltd, Glasgow, UK

[2]Institute of Photonics & Quantum Sciences, School of Engineering and Physical Sciences, Heriot-Watt University, Edinburgh, UK

Correspondence

Ross Donaldson.
Email: r.donaldson@hw.ac.uk

Funding information

Royal Academy of Engineering, Grant/Award Number: RF\201718\1746; Innovate UK, Grant/Award Numbers: TS/S009353/1, TS/T017090/1, TS/W004739/1; Engineering and Physical Sciences Research Council, Grant/Award Number: EP/S022821/1

Abstract

In free-space implementations of Quantum key distribution (QKD), the wide adoption of near-Infrared wavelengths has led to the common use of silicon single-photon avalanche diodes (Si-SPAD) for receiver systems. While the impacts of some SPAD properties on QKD have been explored extensively, the relationship of spot-size and spatial position on the full instrumental response and thus quantum bit error rate (QBER) has been studied little. Changes in spot size and spatial position can result from atmospheric turbulence and pointing and tracking errors. Here, An empirical analysis of that relationship is presented utilising a large active area, 500 μm, free-space coupled Si-SPAD designed for free-space QKD. A baseline full-width at half-maximum timing jitter of 182 ps and a QBER contribution of 0.1 % for a 1 GHz clock frequency QKD system and 100 ps time-gating window are reported. The impacts of spot-size and spatial position can increase the QBER to over 0.3%. The link between the spot-size and timing jitter will allow the understanding of tolerancing for the alignment of Si-SPADs within free-space QKD receiver systems—an important factor in designing properly engineered practical systems and the equipment needed to compensate for atmospheric turbulence and pointing and tracking.

KEYWORDS

optical fibre networks, photons, quantum communication

1 | INTRODUCTION

In recent years, there has been a rapid expansion in the field of quantum communications with the development of new protocols [1, 2], improved components [3, 4], as well as deployment in situ test-beds [5–7]. Quantum key distribution (QKD) [8], an encryption key growing protocol, is the most mature quantum communications technology currently making its transition into commercialisation.

While optical fibre-based networking has been the focus for many QKD implementations [7, 9, 10], it is the free-space links that have proven to be of more interest recently due to the need for last-mile connectivity and global networking capabilities. Various configurations for free-space networking exist, such as point-to-point at ground level [11–13], satellite to ground [14, 15], drones [16], and high-altitude platforms (HAPs) [17]. These free-space implementations still suffer from issues such as atmospheric turbulence [18] and pointing and tracking errors. These errors are reduced in receivers that make use of fibres in their back-end systems, alongside reducing background noise which can make daylight QKD feasible through space, temporal, wavelength filter/selection [19–21]. It is important to note that in this paper, when fibre-based systems are discussed, it is in reference only to the ground-based receiver for a QKD communication network. It is common to use silicon single-photon avalanche detectors (SPADs) for QKD receivers when transmitting in the visible or near-Infrared [22], due to the low dark count rate, moderate detection efficiency, and commercial availability of the detectors. Superconducting nanowire single-photon detectors (SNSPDs) [23] could be an option, however, which boast lower dark count rates and narrower timing jitter [24]; but due to the

need to cryogenically cool the detector to guarantee performance and single-mode coupling, the SPAD has been generally preferred for larger-scale implementation.

Single-photon detectors are a primary driver for the performance of QKD, particularly at high clock frequencies, with dependencies on parameters such as dark count rate, detection efficiency, after-pulsing and in this paper, the timing resolution (typically presented as the full-width at half-maximum (FWHM) time-jitter, but for quantum bit error rate (QBER) considers the full-instrumental response). The timing jitter for a SPAD is the delay between the photon arrival time at the detector and the time it is absorbed by the detector and output electronically as a measurement. The timing jitter places a resolution limit of how fast a QKD system can be operated, so the probability of the incorrect photon being recorded for the key at high operational frequencies is increased [24, 25]. The incoming photons are recorded as a pulse on the detector, and each consecutive photon will overlap with the tail of the previous pulse. How much these pulses overlap will determine how much of an increase to the QBER will be contributed by the timing jitter. Several investigations have characterised smaller active area, low timing jitter, SPADs [26–28] and Si Photomultipliers (SiPMs) [29–31]. All devices showed a full-width at half-maximum timing jitter in the 10's of ps; however, the smaller active area of the SPADs have a much lower detection efficiencies in the near-infrared region, which would result in poor QBER performance for a practical implementation.

Previous works exploring the QBER impact of the timing jitter response of SPADs have primarily focused on the use of the single-mode fibre [24], due to the communities focus on optical fibre networking at the time. There has been a study into the impact of multimode fibres on the QBER at high repetition rates [32]. Modal dispersion within multimode fibres will mean that a larger core size will cause higher losses due to the loss of photons outside the time-gating window, but the impact on timing jitter of a SPAD and the contribution of this to the QBER is relatively unknown.

In this paper, we present empirical measurements to understand the link between multimode core diameters, incident spot diameter and relative spatial position of the spot incident on the active area of a large single pixel 500 μm SPAD. We show that the spatial position and spot size impact the full instrumental response, resulting in an increase in QBER for high repetition rate QKD systems. The results reported here will impact the considerations for the use of multimode fibre coupling in QKD receiver design and will influence the definition of tolerances for both manufacture and system alignment.

2 | EXPERIMENTAL SETUP

The experiment conducted here and outlined in Figure 1 will link the contribution of using fibres to the timing jitter of single-photon detectors and the QBER due to it. Taking measurements with both single-mode and multimode fibres, we can draw conclusions on whether the incident spot size will have an impact, regardless of the number of modes, or it is inherently a multimode fibre contribution.

A free-space Picoquant laser, with an emitting wavelength of 850 nm was used to provide the light source, which was triggered by a pulse generator (repetition rate of 1 MHz) to generate an optical pulse with a pulse width <70 ps. The pulse generator also provided a synchronisation pulse for a time-correlated single-photon counter (TCSPC), which was also used to record the photon time-tags with a 1 ps resolution. The laser output was attenuated from 1 μW down to the single-photon level with a total summated counts of 10^5 counts per second.

The single-photon detector used for these measurements was a single pixel silicon SPAD developed by RedWave Labs, which had a fibre adapter. The detector had a detector active area of 500 μm, a dark count rate of 100 cps, a detection efficiency at 800 nm of 55%, and a stated full width at half-maximum timing jitter of 180 ps at 850 nm.

The SPAD was free space coupled, so for this work, it was required to adapt this to become fibre coupled. By using a focusing block aligned to the front of the SPAD, the spot size on the SPAD will nominally be a $1/e^2$ diameter of 27 μm. The alignment was achieved using a custom rig that provides the ability for the incident beam to be scanned across the active area of the detector. This both aided alignment and allowed measurements to be taken across the full active area of the SPAD.

There was a selection of fibres used for this work: a single-mode fibre and several multimode optical fibres (step-index) of core diameters 10, 50, 105, 200 and 400 μm, respectively. Two multimode optical fibres (graded index) of 50 and 62.5 μm were also included as options with larger core diameters with higher bandwidths. All optical fibres were 1 m in length for this investigation.

Convention is to use a small incident spot size on the SPAD, which will aid with alignment onto active detector diameters of smaller than 500 μm. However, this comes with challenges since micron precision will have to be maintained over long periods of time. This study will help to understand how much of an impact on the time-jitter response of the detector if an incident spot is not so well aligned, or when there is variation in the spot size.

3 | RESULTS

This selection of empirical measurements will help to support the feasibility of multimode fibres to use as fibre coupling in QKD receivers. Firstly, the single-mode response will be reported in terms of the response across the active area. Then, the results from the multimode core diameter measurements will be reported and their impact on the useable area of the SPAD.

3.1 | Single mode response

The incident spot was raster scanned across the surface of the detector in 50 μm increments, and at each step, the timing jitter

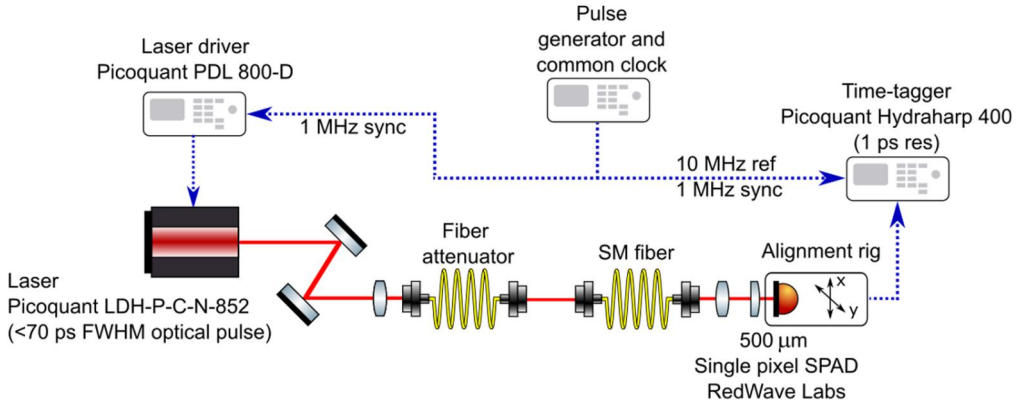

FIGURE 1 Set up for measurement of the spot size response with the single-photon avalanche diodes (SPAD). The laser pulse was generated at 1 MHz repetition rate using a pulse generator with a 10 MHz reference to the time correlated single-photon counter (TCSPC). The laser output was attenuated down to the single-photon level using a fibre attenuator and passed through a SM fibre that were coupled into the SPAD using a fibre collimator. The SPAD was held in an alignment rig with a focusing lens to adjust the collimated beam to the measurement spot sizes. The readout from the SPAD was measured with the time tagger.

was recorded. These results were used to simulate the jitter contribution to the QBER at 1 GHz, such as in [24, 32]. The measurements have mapped out the areas of the detector which have the better response in comparison to other areas.

The map in Figure 2 shows the diameter of the detector with a true active area of 400 µm in diameter. The remaining 50 µm gap either side between the physical edge of the detector and the active area shows an increase in timing jitter as the beam is now incident on the edge of the detector and some back scattering will now be involved in the measurement.

The timing jitter is measured as the full-width half-maximum (FWHM) of the response and the lowest timing jitter recorded was 181 ps, which lies at the centre of the active area of the SPAD. This rises to 280 ps towards the edge of the 400 µm active diameter—which is still comparable with similar commercial off-the-shelf modules, which typically have timing jitter baselines of 350 ps and above, whilst having smaller active areas [33]. At the edge of the detector, the timing jitter rises rapidly to almost double. This mapping shows that if there were a fixed requirement on the QBER for a 1 GHz clock frequency QKD system, then there could be areas of the SPAD that do not meet the requirement, and hence tolerancing of the spatial position can be applied to ensure the performance is always bounded. The increase in timing jitter towards the edge of the SPAD is due to the electric field potential at the wall of the device, causing slower and interrupted propagation of the avalanche.

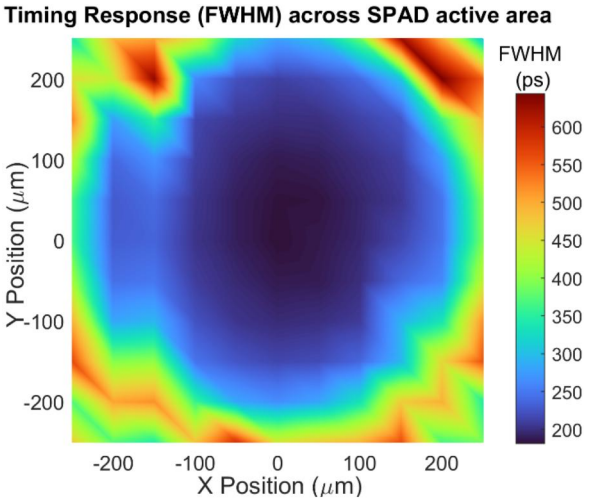

FIGURE 2 A Full 2-D map for timing jitter (FWHM) response on the detector for a SM fibre with an incident spot of $1/e^2$ diameter of 86 µm. This is achieved by scanning the beam across the surface of the detector, with a 50 µm step size, and a measurement using the Hydraharp (time tagger) is recorded at each step.

3.2 | Multimode response

With a fixed distance to the SPAD, multimode fibres with an increasing core size have been measured to get an indication of the performance change across a cross-section of the SPAD detector area. To quantify the incident spot diameter from each of these fibres, each output was imaged using a CMOS camera. The spot diameter has been calculated from the $1/e^2$ value of the response curve. This ensures that the majority of the signal was encapsulated in the measurement, and anything below this level can be considered as background noise in the system.

Figure 3 shows the spot size capture by the CMOS camera at the same distance as the SPAD detection plane would be. The box indicates the 400 µm active area of the SPAD. The smaller core diameters can be seen to fall well within the SPAD active area. Interestingly, the 105 µm appears visually to overfill the detector area—however, the intensity at the $1/e^2$ value falls within the incident spot in the area, and this overfill is measured within the level of background noise. In the 200 and 400 µm images in Figure 3, evidence of defects can be seen round the edges of the fibre connector surface. This is due to the fibres being hand polished and the cladding not being cleaned of epoxy, but it does not affect the fibre core itself.

The sizes of the spot diameter for the multimode fibres are determined by the NA of the fibre, the collimation lens, and the focusing lens at the SPAD interface. All measurements have been taken at the same distance above the SPAD—where the focusing lens to the detector will have the same fixed distance.

To measure the impact of the spatial position, the incident beam was scanned over the full width of the detector at the centre. With an independency of spot size and timing jitter as discussed before, we can assume that the influence on the timing jitter response is related to the properties of multimode fibres. The smaller core diameters have similar responses to the single-mode fibre. These findings have been discussed in a previous piece of work on the influence of core size on timing jitter on a detector [32]. At high repetition rates, for example, 1 GHz, the timing jitter contribution to the overall QBER [34], defined as $QBER_{jitter}$, also deteriorates with a core diameter as seen in Figure 4a.

The 200 and 400 μm core diameter will overfill the detector, due to its large NA and therefore spot diameter, seen in Table 1. However, the results for the 105 μm core diameter has small enough incident spot that we can record a meaningful measurement on the SPAD. As the core diameter increases above 50 μm, then the response of the detector deteriorates in terms of timing jitter.

The full-width tenth maximum (FW10M) and full-width hundredth maximum (FW100M) highlight the influence of the diffusion tail of the minimum timing jitter measured at the centre of the SPAD, outlined in Figure 5. Figure 4b shows that the response along the diffusion tail will affect the jitter greater than at the initial peak of the pulse. As the fibre core diameter increases, the spread of the acceptable timing jitter reduces—this is particularly noticeable for the 105 μm core diameter, which will only allow for a 100–200 μm diameter of the detector that will produce a suitable response, only a 100 μm diameter in the case of the $QBER_{jitter}$ performance as seen in Figure 4a.

The results in Figure 5 show that with a larger core diameter, the tolerance on the spatial position on the SPAD reduces, which begins with the 50 μm step index core diameter.

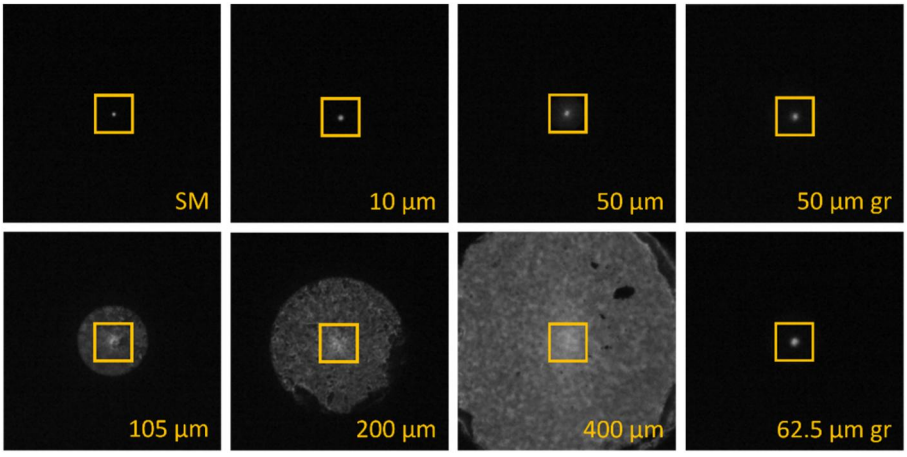

FIGURE 3 Fibre output for each multimode fibre, which shows the incident spot diameter when focused at the detection plane on the single-photon avalanche diodes (SPAD). An indication of the SPAD active area (orange box) is given in each image. Two fibres are the graded index, which are noted using 'gr', and the other six fibres here are the step index.

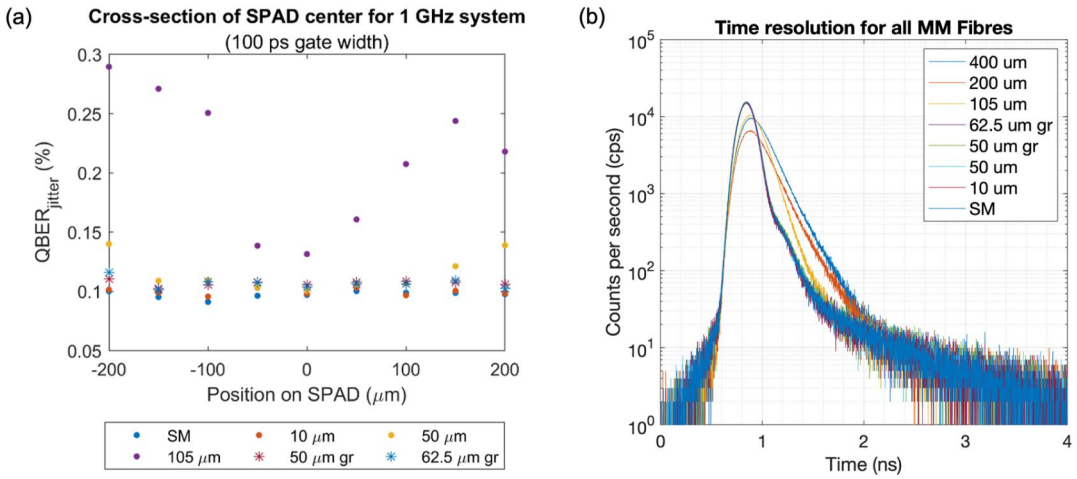

FIGURE 4 (a) A QBER contribution cross-section of the single-photon avalanche diodes (SPAD) centre with a fixed Y position, but a sweep through the centre X positions across the detector surface, for the smaller multimode fibre core diameters. Graded fibre is represented with a dashed line. (b) Measured pulses for the increasing fibre core diameters. As the core diameter increases, the pulse widens, and in turn, lengthens the diffusion tail.

The response of step-index core diameters that lie between 50 and 105 μm would in theory follow the expectation that the useable area would start to reduce increasingly. The graded index fibre equivalents have a similar performance to the single-mode fibre, which has been reflected in previous work [32].

The jump in the performance between 50 and 105 μm core diameter would suggest that these larger core diameters are not suitable for the application in QKD. However, all the core diameters report a jitter of less than the stated timing jitter for the similar Excelitas SPAD, which is 350 ps [33]. This does not mean that these core diameters should be disregarded entirely, as it will need to be considered against the wider design and the stack up of the contributions to the overall QBER of a QKD system, which will be specified by the application requirements. The modelling in this work focuses on high bandwidth, but lower bandwidth will experience less of a QBER impact due to the separation between the optical pulses. Table 2 gives a short example of the core diameter and the area to which it can be aligned within the SPAD detector area when the $QBER_{jitter}$ is required to be below a certain value. This can be adjusted depending on requirements, which will differ between applications.

TABLE 1 Corresponding spot diameter incident on single-photon avalanche diodes (SPAD) with associated fibre NA. The spot diameter has been measured using a CMOS sensor and the $1/e^2$ value calculated.

Core diameter (μm)	NA	Spot diameter on SPAD (μm)
5 (SM)	0.13	27
10	0.1	42
50	0.22	131
105	0.22	351
200	0.22	599
400	0.5	1330
50 (graded)	0.2	74
62.5 (graded)	0.275	59

4 | DISCUSSION

The convention has always been to focus the spot incident onto a SPAD to be as small as possible to ensure a suitable response from the detector. However, it can be seen that the response can accommodate the change in the spot diameter and spatial position to a large degree. This is noticeable particularly towards the edge of the detector area where it would be expected to degrade in performance. As quantum communication and QKD devices seek to become more practical and affordable, understanding the tolerances and impact on performance will be critical to the manufacturing and design process for both free-space and fibre-coupled systems. With respect to free-space coupled systems, the requirements on the turbulence mitigation and pointing and tracking system can be defined without over specification—saving costs. With respect to the fibre-coupled systems, it is the manufacturing tolerance on positioning in both the focus and spot position plane—if this can be relaxed, the time and effort of manufacture may reduce.

The larger core diameters are a concern for the timing jitter of any SPAD, but it is possible to see the impact that it will have across the full active area. In this regard, it gives an indication of, when moving to larger core diameters, how

TABLE 2 Example of the useable detection area for the single-photon avalanche diodes (SPAD) when the requirements identify a contribution to the QBER from the jitter of less than 0.2% at a 1 GHz repetition rate.

Active area (μm)	Fibre core diameter (μm)	Timing jitter (ps)	$QBER_{jitter}$ (%)	Useable area for required $QBER_{jitter}$ of <0.2% (μm)
500	50	190–300	0.1–0.14	±200 from centre
500	105	250–310	0.13–0.29	±50 from centre

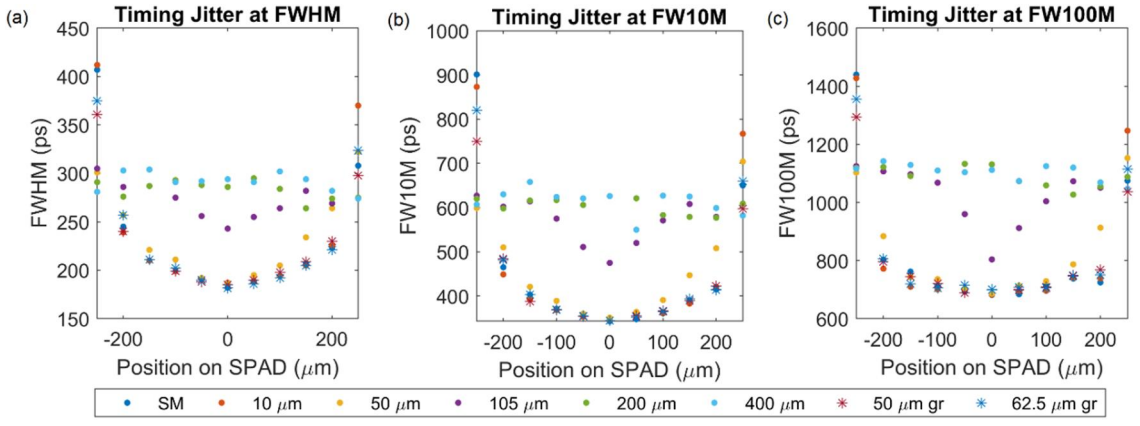

FIGURE 5 Timing jitter for all multimode fibre core diameters for the (a) FWHM, the (b) FW10M and the (c) FW100M. Dots and asterisks represent step-index fibres and graded fibres, respectively.

much tighter alignment tolerances on the SPAD would need to be to ensure that the timing jitter will not over-contribute to the QBER of the overall receiver system. This is due to the fact that since the core is larger, more light can be coupled into the system, but with this there is also larger levels of noise. This would need to be considered in terms of trade-off for the design and of what levels of noise can the system tolerate.

In terms of the receiver design, coupling SPADs to the receiver system using fibre can alleviate some concerns such as mass, space and thermal considerations which can make it easier to implement. The challenges will lie in the alignment of the system, which will depend on guaranteeing a quality of coupling efficiency into these fibres. This will depend on the delivery of the signal to the SPADs before the fibre coupling. In a free-space system, this will entirely depend on the beam correction in the system. But the results here can give an indication that the SPAD can equally perform with a selection of different spot diameters incident on the active area of the detector. For free-space performance, this will place a requirement on the pointing and tracking systems to ensure that the incident spot diameter is at least smaller than the active area of the detector to guarantee a detection.

5 | CONCLUSION

With free-space QKD channels being a victim to variable channel loss and limited communication windows, understanding the performance when operating at high operational frequencies is critical. This paper presents an experimental analysis of an area that is important in the implementation of QKD at high repetition rates, 1 GHz as this is more indicative of a use-case situation. Here, the 500 μm SPAD recorded a timing jitter of 182 ps which relates to a QBER contribution as low as 0.1%, which can allow for 400 μm of the active area to be utilised for single-photon measurements.

The results show that large core diameters will increase the timing jitter of the detector, and as we increase above 105 μm range, then the detector will be overfilled. Development of larger detectors could allow for these larger core diameters to give a true indication of contribution to timing jitter in the future. It should be noted that the 500 μm active area SPAD used in this case has a better baseline performance that is smaller off the shelf modules such as the 180 μm Excelitas SPAD. This is a positive result in the fact that by using these detectors, there is more allowance for the adjustment onto the SPAD, which in turn could make it more suitable for commercial QKD systems.

As reported in a previous study [32], the graded-index fibres allow for larger core diameter to be used, without the performance suffering in comparison to when the system is coupled with a much smaller single-mode fibre. This flexibility in using different core sizes without performance loss is positive knowledge for simplifying the alignment process for future commercial systems.

The impact of the changing spot diameter incident on the detector due to the change in the multimode fibre core diameter will influence the timing jitter, which in turn influences the $QBER_{jitter}$, as seen in the example outlined in Table 2. This in turn impacts manufacturing tolerancing considerations for alignment of the SPADs to QKD receiver systems, whether directly free-space or fibre-coupled. Alignment tolerances are important in terms of design since it will directly influence the requirements for pointing and tracking systems as well as lower-level beam stability through a receiver. The results presented here can be used to aid the requirements of tolerances for systems which will set the standards for manufacturing a commercial-based receiver.

The work here also highlights the need for characterisation at the system level to fully understand the performance before it is deployed for operation. The $QBER_{jitter}$ is a small contribution to a much larger QBER stack up through the system. This will need to be a consideration right through to the commercialisation of a system.

AUTHOR CONTRIBUTIONS

Alexandra Lee: Conceptualisation; data curation; formal analysis; investigation; methodology; validation; visualisation; writing – original draft; writing – review & editing. **Alfonso Tello Castillo**: Software; writing – review & editing. **Craig Whitehill**: Supervision; writing – review & editing. **Ross Donaldson**: Funding acquisition; supervision; writing – review & editing.

ACKNOWLEDGEMENTS

We would like to acknowledge Dmitri Permogorov and the team at RedWave Labs for the use of a SPAD in this investigation. This work was supported by the UKRI EPSRC Centre for Doctoral Training in Applied Photonics [EP/S022821/1]; Innovate-UK through projects TS/S009353/1, TS/T017090/1, & TS/W004739/1; and the Royal Academy of Engineering through an Early Career Research Fellowship No. RF\201718\1746.

CONFLICT OF INTEREST STATEMENT

The authors declare no conflict of interest.

DATA AVAILABILITY STATEMENT

Data available on request.

ORCID

Alexandra Lee https://orcid.org/0000-0003-2478-376X
Ross Donaldson https://orcid.org/0000-0002-6450-1889

REFERENCES

1. Donaldson, R.J., et al.: Experimental demonstration of kilometer-range quantum digital signatures. Phys. Rev. A. Coll. Park. 93(1), 012329 (2016). https://doi.org/10.1103/physreva.93.012329
2. Xu, F., et al.: Experimental quantum fingerprinting with weak coherent pulses [Internet]. Nat. Commun. 6(1), 8735 (2015). https://doi.org/10.1038/ncomms9735
3. Morrison, C.L., et al.: A bright source of telecom single photons based on quantum frequency conversion [Internet]. Appl. Phys. Lett. 118(17), 174003 (2021). https://doi.org/10.1063/5.0045413
4. Korzh, B., et al.: Demonstration of sub-3 ps temporal resolution with a superconducting nanowire single-photon detector [Internet]. Nat.

Photonics 14(4), 250–255 (2020). https://doi.org/10.1038/s41566-020-0589-x
5. Collins, R.J., et al.: Experimental demonstration of quantum digital signatures over 43 dB channel loss using differential phase shift quantum key distribution [Internet]. Sci. Rep. 7(1), 3235 (2017). https://doi.org/10.1038/s41598-017-03401-9
6. Huang, Z., et al.: Experimental implementation of secure anonymous protocols on an eight-user quantum key distribution network. Npj Quan. Inf 8(1), 25 (2022). https://doi.org/10.1038/s41534-022-00535-1
7. Chen, Y.A., et al.: An integrated space-to-ground quantum communication network over 4,600 kilometres [Internet]. Nature 589(7841), 214–219 (2021). https://doi.org/10.1038/s41586-020-03093-8
8. Pirandola, S., et al.: Advances in quantum cryptography. Adv. Opt. Photon. 12(4), 1012–1236 (2020). https://doi.org/10.1364/aop.361502
9. Sasaki, M.: Quantum networks: where should we be heading? [Internet]. Quantum Sci. Technol. 2(2), 020501 (2017). https://doi.org/10.1088/2058-9565/aa6994
10. Sasaki, M., et al.: Quantum photonic network: concept, basic tools, and future issues. IEEE J. Sel. Top. Quant. Electron. 21(3), 49–61 (2015). https://doi.org/10.1109/jstqe.2014.2369507
11. Ursin, R., et al.: Entanglement-based quantum communication over 144km. Nat. Phys. 3(7), 481–486 (2007). https://doi.org/10.1038/nphys629
12. Basso Basset, F., et al.: Daylight entanglement-based quantum key distribution with a quantum dot source [Internet]. Quantum Sci. Technol. 8(2), 025002 (2023). https://doi.org/10.1088/2058-9565/acae3d
13. Noblet, Y., Donaldson, R.: BB84 quantum key distribution transmitter utilising broadband sources and a narrow spectral filter [Internet]. Opt Express 31(9), 15145 (2023). https://doi.org/10.1364/oe.487424
14. Liao, S.K., et al.: Satellite-to-ground quantum key distribution. Nature 549(7670), 43–47 (2017). https://doi.org/10.1038/nature23655
15. Bedington, R., Arrazola, J.M., Ling, A.: Progress in satellite quantum key distribution. NPJ Quan. Inf. 3(1), 30 (2017). https://doi.org/10.1038/s41534-017-0031-5
16. Conrad, A., et al.: Drone-based quantum key distribution (QKD). Hemmati H., Boroson, D.M., editors. 11678:177–184. (2021) https://www.spiedigitallibrary.org/conference-proceedings-of-spie/11678/116780X/Drone-based-quantum-key-distribution-QKD/10.1117/12.2582376.full
17. Chu, Y., et al.: Feasibility of quantum key distribution from high altitude platforms [Internet]. Quantum Sci. Technol. 6(3), 035009 (2021). https://doi.org/10.1088/2058-9565/abf9ae
18. Griffiths, R., et al.: Demonstrating 24-hour continuous vertical monitoring of atmospheric optical turbulence. Opt Express 31(4), 6730–6740 (2023). https://doi.org/10.1364/oe.479544
19. Liao, S.K., et al.: Long-distance free-space quantum key distribution in daylight towards inter-satellite communication. Nat. Photonics 11(8), 509–513 (2017). https://doi.org/10.1038/nphoton.2017.116
20. Han, L., et al.: Integrated Fabry–Perot filter with wideband noise suppression for satellite-based daytime quantum key distribution [Internet]. Appl. Opt. 61(3), 812 (2022). https://doi.org/10.1364/ao.447785
21. Avesani, M., et al.: Full daylight quantum-key-distribution at 1550 nm enabled by integrated silicon photonics [Internet]. Npj Quan. Inf 7(1), 93 (2021). https://doi.org/10.1038/s41534-021-00421-2
22. Buller, G.S., Collins, R.J.: Single-photon generation and detection. Meas. Sci. Technol. 21(1), 012002 (2010). https://doi.org/10.1088/0957-0233/21/1/012002
23. Morozov, D.V., Casaburi, A., Hadfield, R.H.: Superconducting photon detectors. Contemp. Phys. 62(2), 69–91 (2021). https://doi.org/10.1080/00107514.2022.2043596
24. Clarke, P.J., et al.: Analysis of detector performance in a gigahertz clock rate quantum key distribution system. New J. Phys., 13 (2011)
25. Hadfield, R.H.: Single-photon detectors for optical quantum information applications. Nat. Photonics 3(12), 696–705 (2009). https://doi.org/10.1038/nphoton.2009.230
26. Nolet, F., et al.: Quenching circuit and SPAD integrated in CMOS 65 nm with 7.8 ps FWHM single photon timing resolution. Instruments 2(4), 19 (2023). https://doi.org/10.3390/instruments2040019
27. Gramuglia, F., et al.: A low-noise CMOS SPAD pixel with 12.1 Ps SPTR and 3 Ns dead time. IEEE J. Sel. Top. Quant. Electron. 28(2), 3800809 (2022). https://doi.org/10.1109/jstqe.2021.3088216
28. Gramuglia, F., et al.: Sub-10 ps minimum ionizing particle detection with geiger-mode APDs. Front. Phys. 10 (2022). https://doi.org/10.3389/fphy.2022.849237
29. Nolet, F., et al.: Digital SiPM channel integrated in CMOS 65 nm with 17.5 ps FWHM single photon timing resolution. Nucl. Inst Methods Phys. Res. 912, 29–32 (2018). https://doi.org/10.1016/j.nima.2017.10.022
30. Nemallapudi, M.V., et al.: Single photon time resolution of state of the art SiPMs. J. Inst. Met. 11(10), P10016 (2016). https://doi.org/10.1088/1748-0221/11/10/p10016
31. Acerbi, F., Gundacker, S.: Understanding and simulating SiPMs. Nucl. Instrum. Methods Phys. Res. 926, 16–35 (2019). https://doi.org/10.1016/j.nima.2018.11.118
32. Lee, A., et al.: Quantum bit error rate timing jitter dependency on multimode fibers. Opt Express 31(4), 6076 (2023). https://doi.org/10.1364/OE.477156
33. Fong, B.S., Davies, M., Deschamps, P.: Timing resolution and time walk in super low K factor single-photon avalanche diode—measurement and optimization. J. Nanophotonics 12(1), 016015 (2018). https://doi.org/10.1117/1JNP12016015
34. Castillo, A.T., Eso, E., Donaldson, R.: In-lab demonstration of coherent one-way protocol over free space with turbulence simulation. Opt Express 30(Issue 7), 11671–11683 (2022). https://doi.org/10.1364/oe.451083

How to cite this article: Lee, A., et al.: The impact of spot-size on single-photon avalanche diode timing-jitter and quantum key distribution. IET Quant. Comm. 5(4), 443–449 (2024). https://doi.org/10.1049/qtc2.12091